The first two lines vanish on account of Eqs. (B16), the third line vanishes because the asymptotic behavior of both $\chi_n^{(-)*}$ and y_n is outgoing, and the fourth line gives rise to a surface term which is equal to the transition matrix elements T_{dp}.[39]

If the feedback of the stripping mechanism upon the deuteron channel is negligible, then the right-hand side of Eq. (B12) can be set equal to zero and the functions f_d can be obtained from a conventional optical-model deuteron potential. However, the case where the analog state has a spectroscopic factor close to unity is interesting because then the coupling term in Eq. (B12) cannot be neglected. In this case, as the incident deuteron energy is varied near the threshold of the analog channel, the opening of the latter should introduce a particular energy dependence in f_D. The energy dependence might in turn reflect itself in the stripping cross section to other channels which are not related to the neutron channel via charge exchange, and the results may differ from those obtained by Tamura and Watson.[15]

[39] A. Messiah, *Quantum Mechanics* (John Wiley & Sons, Inc., New York, 1962), Eq. (XIX.9).

PHYSICAL REVIEW VOLUME 163, NUMBER 4 20 NOVEMBER 1967

Study of the Low Levels of Si^{27}

M. B. Lewis and N. R. Roberson
Duke University, Nuclear Structure Laboratory, Durham, North Carolina

and

D. R. Tilley
North Carolina State University, Raleigh, North Carolina
and
*Duke University, Nuclear Structure Laboratory, Durham, North Carolina**

(Received 7 July 1967)

The low-lying excited levels of Si^{27} have been studied by the $Si^{28}(He^3,\alpha\gamma)Si^{27}$ reaction. The particle-γ angular-correlation method of Litherland and Ferguson was used. Most probable spin assignments for the 0.96-, 2.17-, and 2.65-MeV levels were determined as $\frac{3}{2}$, $\frac{7}{2}$, and $\frac{5}{2}$, respectively. Transitions from the 3.54- and 4.13-MeV levels appeared to have isotropic γ-ray angular correlations, and decayed primarily through the well established $J=\frac{1}{2}$ level at 0.78 MeV. A spin assignment of $\frac{1}{2}$ is likely for these two levels, although a $J=\frac{3}{2}$ assignment cannot be rigorously ruled out. The branching scheme for the decay of the 3.80-MeV level suggests a spin of $\frac{3}{2}$ for this level although an angular correlation was not carried out. The levels at 2.87 and 2.91 MeV were not resolved, and an angular correlation for these levels was not carried out. The γ-ray spectra for the doublet indicate a strong ground-state transition for both levels. Mixing ratios and branching ratios for many of the γ-ray decays were measured for the first nine levels. Strong- and weak-coupling model calculations were carried out, and the results indicate significant evidence for Si^{28} core-excitation configuration in the Si^{27} levels below 3.00 MeV. Many transition properties predicted by the strong-coupling (rotational) model are in conflict with measured values.

I. INTRODUCTION

THE $1d2s$ shell is now a well established mass region in which nuclei manifest collective excitation properties. In particular, the sequence of spins and some of the spectroscopic properties of low-lying levels in many of the odd-A nuclei show a rotational behavior which is at least approximately accounted for by the coupling of a single particle to a statically deformed core as in the Nilsson model.[1–4] In some cases, particularly those in which there is not a large energy gap between the lowest two odd particle levels, the nucleus may be better described in terms of coupling of an odd particle to two or more different states of the core rather than to a statically deformed one. The different states of the core are due to one or more of the core nucleons occupying one of the excited, but low-lying, single-particle states. As Bhatt[4] has pointed out, such a situation might occur in the $1d2s$ shell near the crossing of the 5th and 9th Nilsson orbits. There is some experimental evidence that Ne^{23}, Al^{25}, Mg^{25}, and Al^{27} have their first excited states (orbit 9) separated about 1 MeV or less from their ground state (orbit 5). For example, Thankappan[5] has described some of the properties of the low-lying levels of Al^{27} in terms of a proton hole coupled

* This work was supported in part by the U. S. Atomic Energy Commission.

[1] A. Bohr and B. R. Mottelson, Kgl. Danske Videnskab. Selskab, Mat. Fys. Medd. **27**, No. 16 (1953).

[2] H. E. Gove, in *Proceedings in International Conference on Nuclear Structure*, edited by D. A. Bromley and E. W. Vogt (The University of Toronto Press, Toronto, Canada, 1960).

[3] J. M. Lacambra, D. R. Tilley, and N. R. Roberson, Nucl. Phys. **A92**, 30 (1967).

[4] Kumar H. Bhatt, Nucl. Phys. **39**, 375 (1962).

[5] V. K. Thankappan, Phys. Rev. **141**, 957 (1966).

to the levels of Si^{28}. Another nucleus which might be expected to show similar properties is Si^{27}.

This paper describes a study of some of the excited levels of Si^{27} below 5 MeV by the measurement of α-γ angular correlations following the excitation of the levels by the $Si^{28}(He^3,\alpha)Si^{27}$ reaction. These measurements have led to the assignment of level spins and to the determination of branching ratios and mixing parameters for the de-excitation γ rays. The particle-γ angular-correlation method of Litherland and Ferguson[6] has been used. In the case of the $Si^{28}(He^3,\alpha)Si^{27}$ reaction, the detection of the α particles at 180° allows only the normalization and the mixing ratio to enter the correlation as arbitrary parameters to be determined by the experiment. Energy-level and transition-probability calculations involving coupling of the odd neutron hole to the remaining core were made. One approach was based upon strong coupling of the neutron hole to a deformed core (Bohr and Mottelson[1]). The other approach was based on weaker coupling to an excited core (Thankappan and True,[7] and de-Shalit[8]).

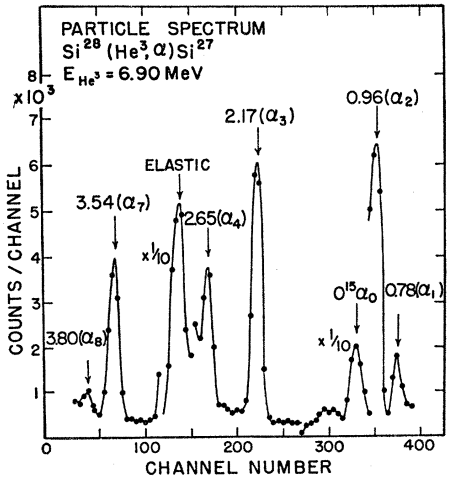

FIG. 1. Particle spectrum in the 180° annular counter from bombardment of a natural silicon target with a 6.9-MeV He^3 beam. The Si^{27} α peaks are identified by the excitation energies and sequence of the levels to which they correspond. The oxygen ground-state group from $O^{16}(He^3,\alpha)O^{15}$ and the Si^{28} elastic group are also labeled.

II. EXPERIMENTAL PROCEDURE

The experiment was performed with the doubly-ionized He^3 beam[9] from the Duke University 4-MeV Van de Graaff. Beam currents of approximately 0.1 μA were obtained at energies up to 8 MeV. The α-γ correlations were measured at bombarding energies of 6.9 and 7.0 MeV, since in this energy region nearly all the low-lying levels of Si^{27} are populated with reasonable strength.

The target was prepared by an electron-gun evaporation of natural silicon (92% isotope purity) onto a thin carbon backing. The carbon backing was found to be necessary in order to give additional support to the target during bombardment by the beam. Several targets with thickness of 50 to 75 $\mu g/cm^2$ were used during the experiment. No α-particle groups from carbon entered the silicon spectrum in the region of interest, and the number of excess γ rays from the reactions with the carbon backing was small compared with those γ rays originating at the collimators.

The α particles were detected by an 80-μ annular surface-barrier counter, which was collimated to detect particles at 175° with respect to the beam direction. The solid angle was chosen such that the half-angle was ±2°. The counter and amplifier system had an intrinsic resolution of 45 keV. An α spectrum recorded with a 6.9-MeV He^3 beam is shown in Fig. 1, while an α spectrum with a 7.0-MeV He^3 beam is shown in Fig. 2. The 7.0-MeV spectrum was recorded with the high-energy α groups off scale, in order to display the groups near α_8 with more resolution. The increase of 100 keV in He^3 energy also increased the yield of the α_8 group. The γ rays were detected by a 3-in.-diam×3-in.-thick NaI crystal mounted on an Amperex 58AVP photomultiplier tube. During some of the earlier measurements a 2-in.×2-in. crystal mounted on a 6810A photomultiplier tube was also used. The front face of the crystal was situated external to the chamber and about 4 in. from the center of the target. The γ-ray counter was moved in 15° or 20° steps from θ=25° to 90°, where θ is measured relative to the beam direction. Measurements

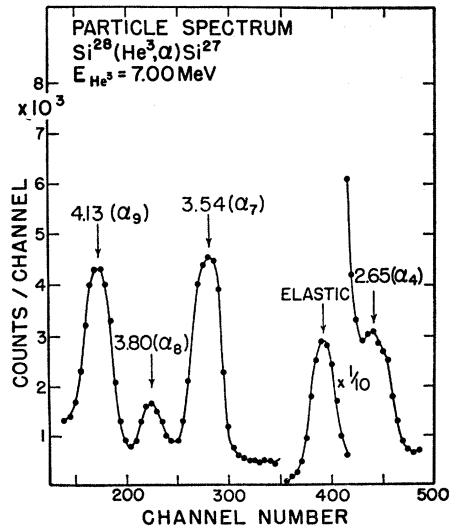

FIG. 2. Particle spectrum in the 180° annular counter from bombardment of a natural silicon target with a 7.0-MeV He^3 beam. The Si^{27} α peaks are identified by the excitation energies and sequence of the levels to which they correspond. The Si^{28} elastic group is also labled.

[6] A. E. Litherland and A. J. Ferguson, Can. J. Phys. **39**, 788 (1961).
[7] V. K. Thankappan and William W. True, Phys. Rev. **137**, 793 (1965).
[8] A. de-Shalit, Phys. Rev. **122**, 1530 (1961).
[9] N. R. Roberson, D. R. Tilley, and H. R. Weller, Nucl. Instr. Methods **33**, 84 (1965).

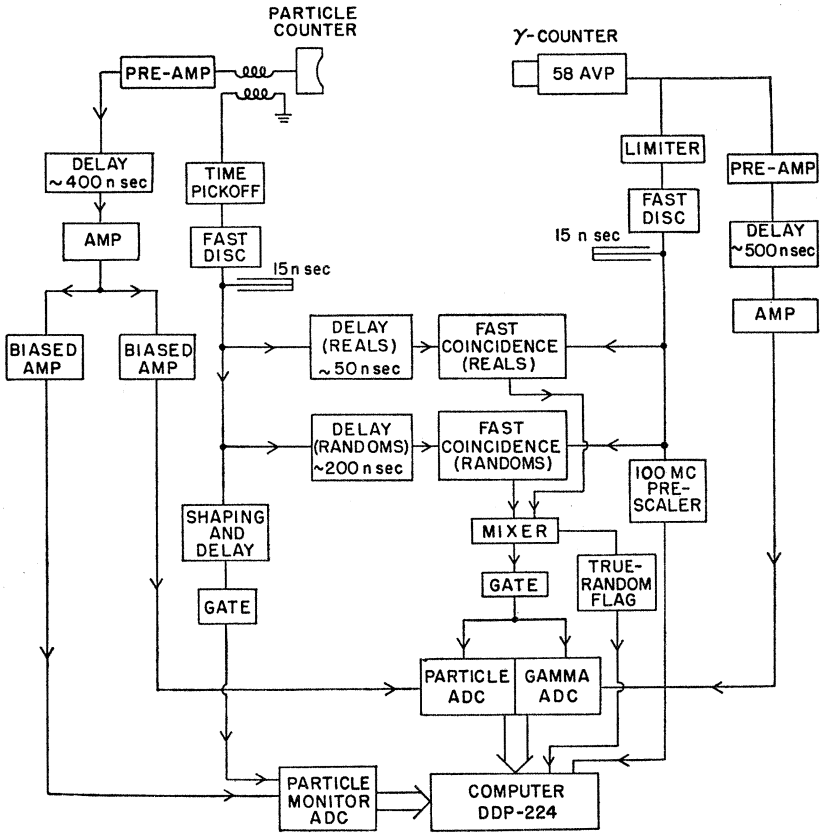

FIG. 3. Block diagram of electronics.

were taken for both positive and negative angles to check for misalignment or for inconsistences in the data points. Running time for each angle was fixed at 4 h. All of the α-γ correlations were repeated two, and for some cases, three times.

The scattering chamber was a 6-in.-diam $\frac{1}{16}$-in.-thick brass shell with a $\frac{3}{8}$-in.-thick bakelite top and bottom. The beam was collimated by a pair of $\frac{1}{16}$-in.-diam tantalum collimators separated by 5 in. The first of these collimators was located 9 in. from the target and was followed by a 3-in.-long solid lead tube which absorbed excess γ rays arising at this collimator. A $\frac{3}{16}$-in.-diam stainless-steel tube which passed through the center hole in the annular counter served as the antiscattering collimator. The Faraday cup was located 60 in. beyond the scattering chamber. At this distance, back scattering from the beam was minimized. The alignment of the chamber and the γ-ray counter was checked by measuring the isotropic correlation for the de-excitation γ rays from the $J=\frac{1}{2}$, 3.09-MeV, state of C^{13} which was excited via the $C^{12}(d,p)C^{13}$ reaction. The deviation from isotropy was less than 2%. The chamber wall transmission was mapped by radiation from a source mounted at the beam spot position.

A schematic diagram of the electronic setup is shown in Fig. 3. Fast rise-time signals were obtained from the surface-barrier detector with a time pick-off circuit, and from the γ-ray detector directly from the anode of the 58AVP. These signals were shaped by fast discriminators and then fed to two fast parallel coincidence circuits, the delay in one being set for true coincidences, the second recording only random coincidences. The resolving times were about 30 nsec and gave a ratio of true to random coincidences for counts underlying the peaks of interest of between 6:1 and 10:1. The pulses from the coincidence circuits were mixed and used to generate gate pulses for the particle and the γ-ray analog-to-digital converters. At the same time a signal was generated which indicated whether the gate was produced by a true or a random event. The digitized outputs of the analog-to-digital converters, along with the true-random flag, were processed by the Duke Nuclear Structure Laboratory on-line computer.[10] The computer was programmed to store and display the true coincidences in a 128×64 channel matrix and simultaneously to record, event by event, both the true and random coincidences on magnetic tape. The particle spectrum was usually stored along the 128-channel axis, and the γ-ray spectrum along the 64-channel axis.

The time pickoff and discriminator network was determined to have a rather broad cutoff resulting in a varying efficiency over part of the particle energy spectrum of interest. The use of low-resistivity (800 Ω

[10] N. R. Roberson, D. R. Tilley, and M. B. Lewis, Bull. Am. Phys. Soc. **10**, 55 (1965). The computer used in the present work was model DDP-224.

cm) surface-barrier detectors reduced, but did not eliminate the problem. Consequently some of the data points, when normalized to the total number of counts in the α counter as determined with a single-channel analyzer, were uncertain by as much as 10%. For these reasons, it was necessary to monitor the efficiency of the particle detector. The linear signal from the annular counter was fanned out to a separate analog-to-digital converter which was gated with the time pickoff and discriminator network. The resulting spectrum was stored and displayed by the computer in a 512-channel array. The number of counts for each α-particle group were then used to normalize the α-γ correlation points. This monitor spectrum was stored on magnetic tape along with the two-parameter data.

To prevent double-pulsing, the γ-ray discriminator was modified to have a fixed 1.5-μsec dead time. Dead time corrections were made by recording with the computer, after prescaling by 10^5, the total number of γ rays. It was found that no corrections greater than 5% were necessary.

After completion of the experiment, the data previously stored on magnetic tape was read back into the computer for further processing. The α-particle peaks in the monitor spectrum which were to be used for normalization were selected and summed with a light pen. A simple point by point summation was made after subtracting a background based on neighboring points which were also selected with the light pen. The true coincidences for each angle were then read from the magnetic tape and summed, event by event, and displayed on the oscilloscope. This latter process is often called delayed-time totalizing. The area corresponding to coincidences between a particular α group and that part of the γ-ray spectrum to be used for the correlation was summed. The random coincidences for the same γ-ray angle were read from the tape and the same area summed. The difference in these numbers, after normalization, represented the true number of events. The analysis program was also used to perform delayed time totalizing of the complete magnetic tape resulting in γ-ray spectra, one for each α-particle group, summed over every angle at which data was taken. These summed spectra are shown in Sec. IV.

III. METHOD OF ANALYSIS

The method of analysis follows closely the linear least-squares fitting procedure discribed by Poletti and Warburton[11] for use with method II of Litherland and Ferguson.[6] The angular distribution of the de-excitation γ rays from a state of spin a to a state with spin b is expressed by

$$W(\theta)=\sum_k \rho_k(a)F_k(a,b,x_{ab})Q_kP_k(\cos\theta)\,, \qquad (1)$$

where θ is the angle between the direction of emission of the γ rays and the axis of alignment, which in this case coincides with the beam axis, the Q_k are attenuation coefficients to account for the finite extent of the detectors and were calculated by numerical methods as suggested by Rose,[12] the $F_k(a,b,x_{ab})$ depend on the γ-ray decay and are independent of the nuclear alignment, the $\rho_k(a)$ are statistical tensors which describe the alignment of the initial state, and $P_k(\cos\theta)$ is a Legendre polynominal.

The statistical tensors $\rho_k(a)$ are given by a sum over the population parameters of the $2a+1$ magnetic substates. That is,

$$\rho_k(a)=\sum_\alpha P(\alpha)\rho_k(a,\alpha)\,, \qquad (2)$$

where $P(\alpha)$ are the population parameters and for an unpolarized state, $P(\alpha)=P(-\alpha)$. In this sum, α takes on values to account for the number of magnetic substates populated in the excited state. For the Si^{28}-$(He^3,\alpha)Si^{27}$ reaction, only the $\alpha=\frac{1}{2}$ substate can be populated since the sum of the spins of Si^{28}, He^3, and α is only $\frac{1}{2}$.

The $F_k(a,b,x_{ab})$ function is given for the case where only the two lowest allowed multipolarities are included by

$$F_k(a,b,x_{ab})=\frac{F_k(LL,ba)+2x_{ab}F_k(LL',ba)+x_{ab}^2F(L'L',ab)}{1+x_{ab}^2}\,, \qquad (3)$$

where $x=\langle b\|L+1\|a\rangle/\langle b\|L\|a\rangle=\pm[\Gamma(E2)/\Gamma(M1)]^{1/2}$ is the mixing ratio and $L'=L+1$. The sign convention used in this work is called convention II by Poletti and Start.[13] For the triple correlation case of $a\rightarrow b\rightarrow c$ in which $a\rightarrow b$ is unobserved, $F_k(a,b,x_{ab})$ is replaced in Eq. (1) by $U_k(a,b,x_{ab})F_k(b,c,x_{bc})$. In this case

$$U_k(a,b,x_{ab})=\frac{U_k(Lab)+x_{ab}^2U_k(L'ab)}{1+x_{ab}^2}\,. \qquad (4)$$

Poletti and Warburton[11] have tabulated the $F_k(LL',ba)$ and $U_k(L,ab)$ coefficients as well as the statistical tensors.

A program using a multiple-regression subroutine performed the least-squares fits using the Duke 7072 computer. The variable used was arctan x, which was varied from $-85°$ to 85° usually in 5° steps. For each value of x the quantity

$$\chi^2=\frac{1}{k-1}\sum_i\frac{[W(\theta_i)-Y(\theta_i)]^2}{[\Delta Y(\theta_i)]^2}\,, \quad i=1 \text{ to } k\,, \qquad (5)$$

was determined, where $Y(\theta_i)$ is the relative yield and $\Delta Y(\theta_i)$ is the statistical error. The most probable values for the spin and mixing ratio x are assumed to be those minimizing χ^2.

[11] A. R. Poletti and E. K. Warburton, Phys. Rev. **137**, 595 (1965).

[12] M. E. Rose, Phys. Rev. **91**, 610 (1953).

[13] A. R. Poletti and D. F. H. Start, Phys. Rev. **147**, 800 (1966).

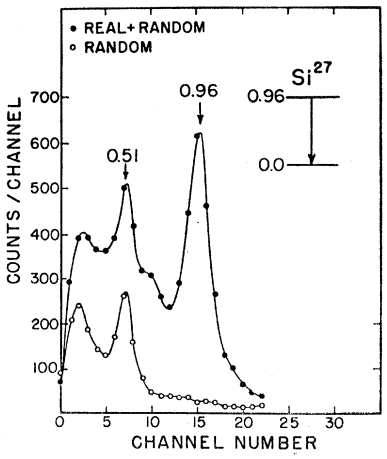

FIG. 4. Spectrum of γ rays summed over five angles in coincidence with the α group populating the Si^{27}-0.96 MeV level in the $Si^{28}(He^3,\alpha)Si^{27}$ reaction at a He^3-energy of 6.9 MeV. The γ-ray peak corresponds to the decay scheme shown. The solid points are the sum of real and random counts. The random counts are indicated by circles. The 0.51 peak consists entirely of random coincidences.

Since the annular particle counter used in this work was not an ideal counter placed at 180° with respect to the beam, magnetic substates with $|\alpha|>\frac{1}{2}$ may be populated to a small extent. From the results of Litherland and Ferguson[6] and for our experimental conditions, it is unlikely that $P(\frac{3}{2})>0.02P(\frac{1}{2})$. One check on this finite size effect was to try to improve the fit for each x by including and varying the values of both $P(\frac{3}{2})$ and $P(\frac{1}{2})$. In no case did the inclusion of $P(\frac{3}{2})$ appreciably improve the fits. A second check was to make consecutive fits to the data, first with $P(\frac{3}{2})=0$ and then with $P(\frac{3}{2})=\xi P(\frac{1}{2})$, where ξ is a small number less than 1.0. Typical results of the finite size effect will be discussed below in Sec. IV.

IV. EXPERIMENTAL RESULTS

A. The 0.78-MeV Level

Hinds and Middelton[14,15] and more recently Swenson, *et al.*[16] have measured the differential cross section for the $Si^{28}(He^3,\alpha)Si^{27}$ reaction leading to the first excited state at 0.78 MeV. Both studies conclude that $l_n=0$ neutron pickup is the correct reaction mechanism, and therefore $J=\frac{1}{2}$ is the spin assignment for the 0.78-MeV level. The γ angular distribution as measured during this experiment was isotropic to within 6% and is consequently consistent with $J=\frac{1}{2}$. Since the angular-correlation technique being used cannot measure the mixing parameter in such a case, no attempt was made to obtain a smaller statistical error for this rather weakly excited state.

B. The 0.96-MeV Level

The summed γ-ray spectrum for the decay of the 0.96-MeV level is shown in Fig. 4. The spectrum is shown without the randoms subtracted. The random spectrum is also shown for comparison as a typical case. The measurements were made at an incident He^3 energy of 6.9 MeV. The possibility of a 0.18-MeV transition through the first excited state at 0.78 MeV could not be determined by the presence of a 0.18-MeV γ ray in this spectrum since the γ discrimination level was set at about 200 keV. Consequently, the 0.78-MeV γ ray was searched for by subtraction of the higher energy 0.98-MeV γ rays. The subtraction of contributions of higher-energy γ rays and the unfolding of photopeaks were facilitated by standard spectral shapes obtained from radioactive sources and from coincidence spectra obtained in work on C^{13} and Si^{29}. No clear evidence for a branch could be found, however. The upper limit to the transition probability for decay through the 0.78-MeV level is about 5%.

The results of the angular correlation are given in Fig. 5, which gives χ^2-versus-arctan x curves for spin assignments of $\frac{3}{2}$, $\frac{5}{2}$, $\frac{7}{2}$, and $\frac{9}{2}$. The validity numbers indicated on the right-hand side of the χ^2 plot represent the probability of χ^2 exceeding these values for a good

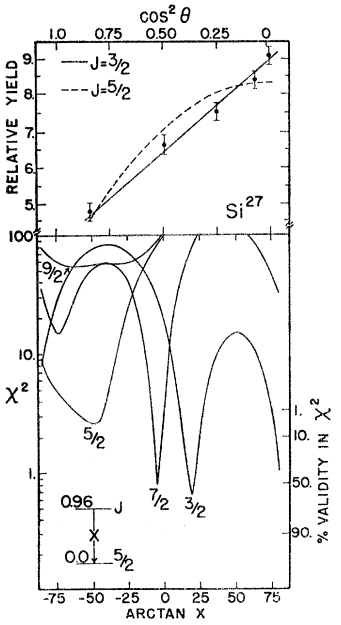

FIG. 5. Angular correlation results for the Si^{27} $0.96 \rightarrow 0$ transition. The lower part of the figure shows χ^2-versus-arctan x curves for assumed spins $\frac{3}{2}$, $\frac{5}{2}$, $\frac{7}{2}$, $\frac{9}{2}$ for the 0.96-MeV level. The percent validity in the values of χ^2 is indicated by the corresponding scale on the lower right. Corrections for finite size are negligible. The upper part of the figure shows the experimental angular-correlation data and the theoretical best fits for the two most probable spins for values of x corresponding to the minimum values of χ^2.

[14] S. Hinds and R. Middleton, Proc. Phys. Soc. (London) **75**, 444 (1960).
[15] S. Hinds and R. Middleton, Proc. Phys. Soc. (London) **73**, 727 (1959).
[16] L. W. Swenson, C. M. Fou, and R. W. Zurmuhle, Bull. Am. Phys. Soc. **11**, 334 (1966).

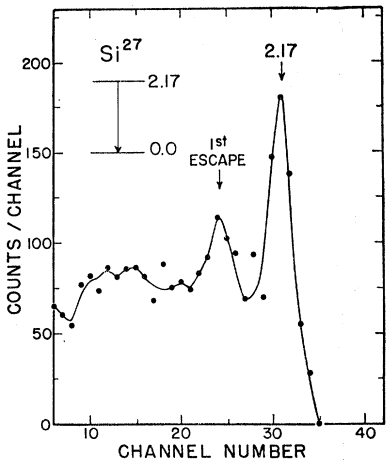

FIG. 6. Spectrum of γ rays summed over five angles in coincidence with the α group populating the Si^{27} 2.17-MeV level in the $Si^{28}(He^3,\alpha)Si^{27}$ reaction at a He^3 energy of 6.9 MeV. The γ-ray peak corresponds to the decay scheme shown. The random coincidences have been subtracted.

solution. The experimental angular distributions and the calculated distributions using the most probable mixing ratio x are shown in the upper part of the Fig. 5. The measured distribution is clearly inconsistent with $J=\frac{9}{2}$, but allows an assignment of $J=\frac{3}{2}$, $\frac{5}{2}$, or $\frac{7}{2}$. The χ^2 curves were quite insensitive to finite size effects. Angular-distribution measurements[14,16] indicate an $\ell_n=2$ pickup reaction mechanism, and this fact rules out the $J=\frac{7}{2}$ possibility. From the remaining curves, it is seen the $J=\frac{3}{2}$ is more than six times as likely as $J=\frac{5}{2}$. In addition, if $J=\frac{5}{2}$, then the mixing ratio for the $0.96\rightarrow 0$ transition is greater than 1.4. This is more than 10^4 times the single-particle Weisskopf estimate and is quite large for nuclei in this mass region. $J=\frac{3}{2}$ with two solutions $x=+(0.36\pm0.03)$ or $x>+6.0$ appears to be the correct assignment for the 0.96-MeV level.

The two solutions for x corresponding to $J=\frac{3}{2}$ indicated above represent a common difficulty since the fitting procedure usually has double-valued solutions, one of which gives a very large mixing ratio. Lifetime measurements are sometimes useful in determining the correct solution. These measurements are not available for the levels of Si^{27}, but several are available for Al^{27}. Using the systematics of other nuclei in this mass region as summarized by Wilkinson,[17] the smaller ratio of $x=+(0.36\pm0.03)$ appears to be most probable.

C. The 2.17-MeV Level

The summed γ-ray spectrum for the decay of the 2.17 level is shown in Fig. 6. The spectrum is shown after subtraction of the random events and was obtained for an incident He^3 energy of 6.9 MeV. The full-energy and first-escape peaks of the $2.17\rightarrow 0$ transition are apparent in this figure, while no other strong transitions are seen. However, when a standard spectrum was used to fit the 2.17-MeV γ rays, a small, but finite, number of counts remained in the region of 0.78 and 0.96 MeV. Assuming that these counts were due to branching through the 0.78- and 0.96-MeV levels it was estimated that the upper limit for each branch was 4%. The absorption efficiencies used in this work were taken from the tabulation by Heath.[18]

The χ^2 computer fit to the angular distribution of the 2.17-MeV γ ray is shown in Fig. 7 for assumed spins of $J=\frac{3}{2}$, $\frac{5}{2}$, $\frac{7}{2}$, and $\frac{9}{2}$. It is seen that the assignments of $J=\frac{5}{2}$ and $\frac{9}{2}$ are in strong disagreement with the measured distribution. The solution to $J=\frac{3}{2}$ is barely outside the 0.1% limit for χ^2. The finite size effect was investigated by calculating χ^2 for $P(\frac{3}{2})=0.05P(\frac{1}{2})$ and this only makes the fit worse. For this reason, we reject $J=\frac{3}{2}$ and accept the $J=\frac{7}{2}$ solution for which $x=-(0.43\pm0.04)$. The $J=\frac{7}{2}$ spin assignment is also consistent with the absence of a strong branch through the $J=\frac{1}{2}$ level at 0.78 MeV or through the $J=\frac{3}{2}$ level at 0.96 MeV.

D. The 2.65-MeV Level

Figure 8 shows the summed γ-ray spectrum for the decay of the 2.65-MeV level recorded with an incident

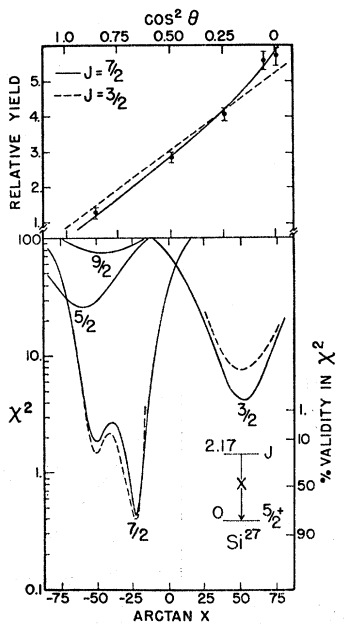

FIG. 7. Angular correlation results for the Si^{27} $2.17\rightarrow 0$ transition. The lower part of the figure shows χ^2-versus-arctan x curves for assumed spins $\frac{3}{2}$, $\frac{5}{2}$, $\frac{7}{2}$, $\frac{9}{2}$ for the 2.17-MeV level. The percent validity in the value of χ^2 is indicated by the corresponding scale on the lower right. The change in the curve shapes near their minima for a finite size correction $P(\frac{3}{2})=0.05P(\frac{1}{2})$ is indicated by the broken curves. The upper part of the figure shows the experimental angular-correlation data and the theoretical best fits for the two most probable spins for values of x corresponding to the minimum values of χ^2.

[17] D. H. Wilkinson, in *Nuclear Spectroscopy*, edited by F. Ajzenberg-Selove (Academic Press Inc., New York, 1960), Part B, p. 858 ff.

[18] R. L. Heath, Phillips Petroleum Company, Atomic Energy Division Report No. IDO-16880-1 (unpublished).

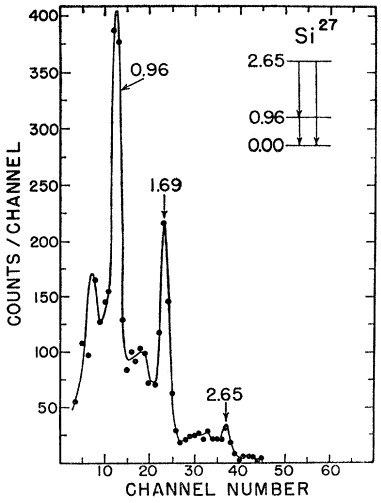

FIG. 8. Spectrum of γ rays summed over five angles in coincidence with the α group populating the Si^{27} 2.65-MeV level in the $Si^{28}(He^3,\alpha)Si^{27}$ reaction at a He^3 energy of 6.9 MeV. The γ-ray peaks correspond to the decay scheme shown. The random counts have been subtracted. The smaller number of counts below channel number 8 is due a high discriminator setting as explained in the text.

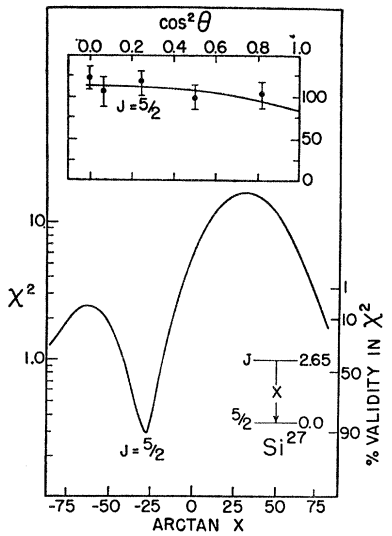

FIG. 10. Angular-correlation results for the Si^{27} $2.65 \rightarrow 0$ transition. The lower part of the figure shows χ^2-versus-arctan x curve for a spin of $\frac{5}{2}$ for the 2.65-MeV level. Corrections for finite size are negligible. The upper part of the figure shows the experimental angular-correlation data and the theoretical best fit for the spin choice $\frac{5}{2}$ corresponding to the minimum value of χ^2.

He^3 energy of 6.9 MeV. The branch through the second excited state at 0.96 MeV and to the ground state were the only ones observed. The shape of the spectrum below 0.96 MeV is due to the fact that the fast discriminator level was set rather high for this run. Supplementary measurements made with lower discriminator settings and with a smaller crystal failed to show any evidence of other transitions. Correct branching ratios are obtained by determining the relative intensities for each branch from the γ-ray angular distributions. These relative intensities together with the absorption efficiencies determine the branching probabilities. Because of the small number of total counts in the full-energy peak, it was necessary to include all counts above about 1.75 MeV, i.e., an appreciable fraction of the compton scattering, in the angular correlation for the $2.65 \rightarrow 0$ transition. After unfolding the higher-energy γ rays, the correlations for the $2.65 \rightarrow 0.96$ and for the $0.96 \rightarrow 0$ transition were composed only of counts in the full-energy peaks. Using the relative intensities and estimating the fraction of the compton scattering included in the ground-state transition, the branching ratios were measured as 18 and 82% for the $2.65 \rightarrow 0$ and $2.65 \rightarrow 0.96$ transitions, respectively. A second calculation was made by assuming that the summed spectrum was approximately equivalent to an angle-integrated one. The areas under the full-energy peaks were used yielding the ratios 23 and 77%. The result for the branching ratio was taken as the average of the two calculations, (20 ± 5) and (80 ± 5)%. As a check on our methods the relative intensity of the 0.96- and 1.69-MeV γ rays was calculated as (0.90 ± 0.05)%, which was considered satisfactory since the counts in the 0.96-MeV photopeak were the result of unfolding two higher-energy γ rays.

Because of poor statistics, the angular correlation of the $2.65 \rightarrow 0$ decay did not restrict the spin of the 2.65-MeV level. It was necessary to use the measurements made on the relatively strong $2.65 \rightarrow 0.96$ and $0.96 \rightarrow 0$ transitions. The results are shown in Fig. 9. The left side of the figure corresponds to the 1.69-MeV γ-ray distribution while the right side corresponds to the 0.96-MeV distribution. Spin choices of $\frac{1}{2}$, $\frac{7}{2}$, and $\frac{9}{2}$ are

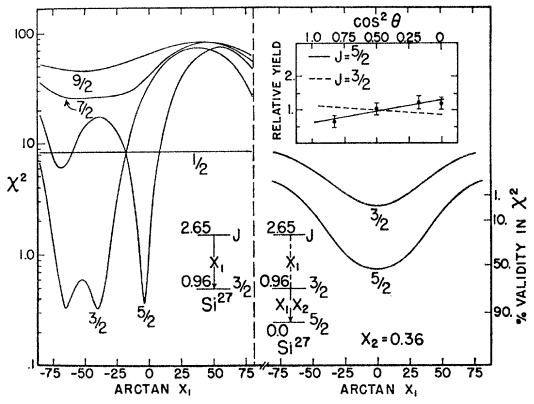

FIG. 9. Angular-correlation results for the Si^{27} $2.65 \rightarrow 0.96 \rightarrow 0$ transitions. The left half of the figure shows χ^2-versus-arctan x_1 curves for assumed spins $\frac{1}{2}$, $\frac{3}{2}$, $\frac{7}{2}$, $\frac{9}{2}$ for the 2.65-MeV level. The percent validity in the value of χ^2 is indicated by the corresponding scale on the extreme right. Corrections for finite size are negligible. The right half of the figure shows the results for the $0.96 \rightarrow 0$ transition following the $2.65 \rightarrow 0.96$ one. The χ^2 scale is the same as that used on the left half of the figure. The upper right part of the figure shows the experimental angular-correlation data and the theoretical best fits for the two most probable spins for values of x_1 corresponding to the minimum values of χ^2 determined by the right half of the figure.

ruled out by the 1.69-MeV correlation. The 0.96 distribution is dependent upon the mixing ratio x_1 of the 1.69-MeV transition populating it as well as the mixing ratio x_2 of the $0.96 \rightarrow 0$ transition. Taking $x_2 = 0.36$ as determined in Sec. IVB and using the triple correlation expression, the χ^2 plot on the right side of Fig. 9 was obtained. The results indicate that $J = \frac{5}{2}$ is the more probable choice of the spin, both because of the small value of χ^2 and the fact that only for $J = \frac{5}{2}$ do the minima in both plots occur for nearly the same mixing ratio ($x_1 \approx 0$). The value of $x_1 = -(0.06 \pm 0.04)$ taken from the 1.69-MeV distribution was assumed to be the correct solution for $J = \frac{5}{2}$. The fit to the 0.96-MeV distribution calculated with the x_1 value measured from the 1.69-MeV distribution is shown at the top right of Fig. 9. Having assigned the spin of the 2.65-MeV level as discussed above, the χ^2 fit for the $2.65 \rightarrow 0$ transition was calculated for $J = \frac{5}{2}$ and is shown in Fig. 10. The mixing ratio was determined to be $x = -(0.50 \pm 0.20)$. The $J = \frac{5}{2}$ assignment spin is also consistent with the $\ell_n = 2$ measurement by Swensen *et al.*[16] for the ^{28}Si-(He^3,α)Si^{27} reaction.

E. The 2.87- and 2.91-MeV Levels

A study of the (α,γ) angular correlation for the fifth and sixth excited state of Si^{27} at 2.87 and 2.91 MeV was complicated by the fact that the groups were not resolved from each other or from the He^3 elastic group.

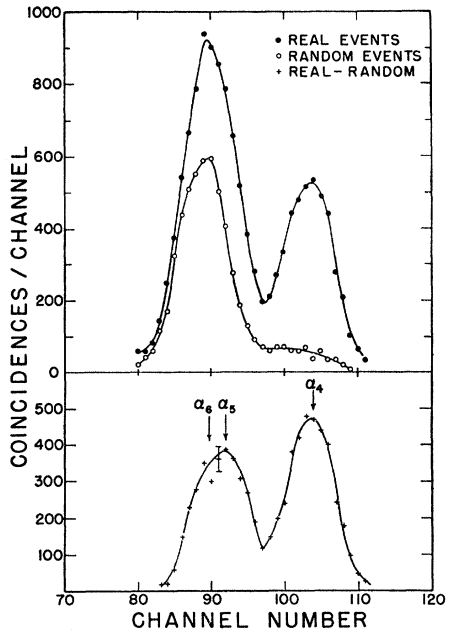

FIG. 11. Summed coincidence spectrum projected onto the particle axis of the α-γ two-dimensional spectrum. At the top of the figure, the real and random counts are shown for comparison. The large random event peak is due to the elastic-scattering peak in the particle spectrum. A subtraction of random from real counts is given with a typical error bar in the lower half of the figure. α groups 4, 5, 6 populating the 2.65-, 2.87-, and 1.92-MeV levels, respectively, are indicated.

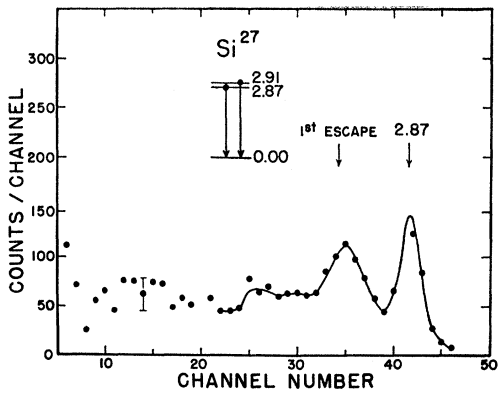

FIG. 12. Spectrum of γ rays summed over five angles in coincidence with the α groups populating the Si^{27} 2.87- and 2.91-MeV levels in the Si^{28}(He^3,α)Si^{27} reaction at a He^3 energy of 7.0 MeV. The γ-ray peak corresponds to the decay scheme shown. The random counts have been subtracted.

This situation is illustrated in Fig. 11. The data were recorded with an incident He^3 energy of 7.0 MeV. Here, the summed coincidence spectrum was projected onto the particle axis in the region of the elastic-scattering peak. The α_5 and α_6 groups are resolvable from the elastic group only after the random coincidences are subtracted. Due to poor statistics resulting from the random coincidences under the elastic peak it was difficult to accurately unfold the α_5 and α_6 peaks separately. The relative strengths of α_5 and α_6 were apparently comparable. The summed spectrum shown in Fig. 12 indicates that a ground-state transition is the primary one for both groups. Due to the uncertainty in the relative strengths of α_5 and α_6, the α-γ correlation was not considered reliable.

F. The 3.54-MeV Level

The (α-γ) correlation for the seventh excited state at 3.54 MeV was measured at bombarding energies of 6.9 and 7.0 MeV. The summed γ spectrum with randoms subtracted is shown in Fig. 13 for a bombarding energy

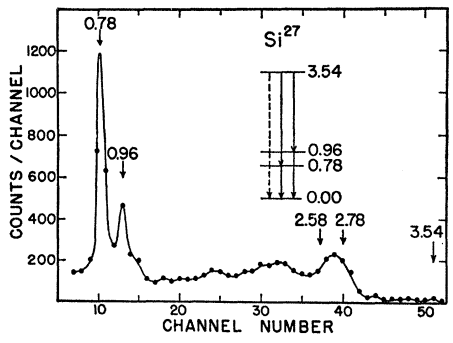

FIG. 13. Spectrum of γ rays summed over five angles in coincidence with the α group populating the Si^{27} 3.54-MeV level in the Si^{28}(He^3,α)Si^{27} reaction at a He^3 energy of 6.9 MeV. The γ-ray peaks correspond to the decay scheme shown. The broken arrow in the decay scheme indicates a very weak or uncertain decay. The random coincidences have been subtracted.

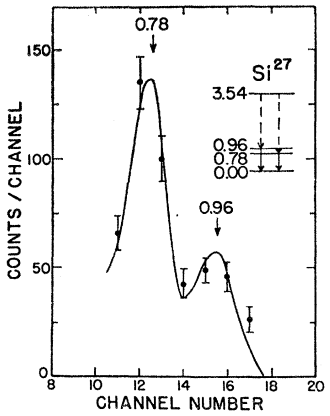

FIG. 14. Spectrum of γ rays in the region of 1 MeV summed over four angles in coincidence with the α group populating the Si^{27} 3.54-MeV level in the $Si^{28}(He^3,\alpha)Si^{27}$ reaction at a He^3 energy of 6.9 MeV. The solid circles represent the data after subtracting out the contribution of the higher-energy γ rays. The γ-ray peaks correspond to the transitions shown by the solid lines. The least-squares fit as discussed in the text is also shown.

of 6.9 MeV. The 3.54-MeV level appears to decay completely through the 0.78- and 0.96-MeV levels. While the 2.58- and 2.76-MeV γ rays and their escape peaks could not be resolved, it was still possible to use standard γ-ray shapes to subtract out the contribution of these high-energy γ rays from under the 0.78- and 0.96-MeV photopeaks. The small but finite number of counts appearing up to 3.54 MeV are probably due to pileup in the γ-ray counter because of the high counting rate. This effect has been seen in other γ-ray spectra in which the residual counts often extend beyond the excitation energy of the particular state.

Since angular distributions for the $0.78 \rightarrow 0$ and $0.96 \rightarrow 0$ transitions are isotropic to within 5%, and since the mixed distribution for the $3.54 \rightarrow 0.96$ and $3.54 \rightarrow 0.78$ transitions is isotropic to within 3%, the branching ratios can be calculated correctly from the summed spectrum. The shape and position of the monoenergetic γ ray from the $0.96 \rightarrow 0$ transition has already been obtained (Sec. IVB), and this spectrum

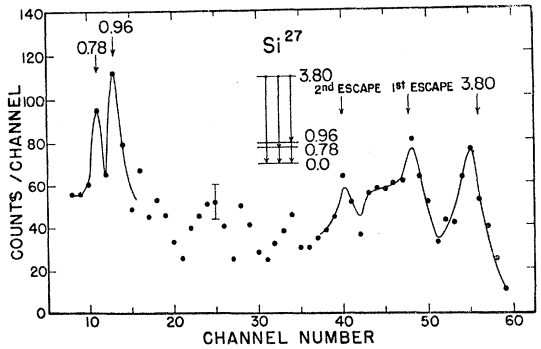

FIG. 15. Spectrum of γ rays summed over five angles in coincidence with the α group populating the Si^{27} 3.80-MeV level in the $Si^{28}(He^3,\alpha)Si^{27}$ reaction at a He^3 energy of 7.0 MeV. The γ-ray peaks correspond to the decay scheme shown. The random coincidences have been subtracted.

was fitted by a least-squares program to the equation

$$y(x)=\exp(a_0+a_1x+a_2x^2)+\exp(b_0+b_1x+b_2x^2), \quad (6)$$

where x is a channel number. The coefficients were determined to give a smooth fit to the photopeak and the high-energy portion of the Compton distribution. A new function

$$Y(x)=T_{0.96}y(x)+T_{0.78}y(ax), \quad (7)$$

where a is a gain factor to account for the different energy of the two peaks, was then fitted by a least-squares program to the 0.78-and 0.96-MeV γ rays as extracted from the summed spectrum for the decay of the 3.54-MeV level. The amplitudes T were determined, and after the relative efficiencies were taken into account the branching ratios of (60 ± 7) and $(40\pm7)\%$ were calculated for the $3.54 \rightarrow 0.78$ and $3.54 \rightarrow 0.96$ transitions, respectively. Figure 14 shows the results of the least-squares fit to the 0.78- and 0.96-MeV γ rays.

The degree of isotropy (3%) of the angular correlation for the mixed transitions suggest that both components in the radiation are nearly isotropic, which would imply $J=\frac{1}{2}$. Calculations were made to see if the isotropy of the unresolved pair could be produced by superimposing the two angular distributions from $3.54 \rightarrow 0.96$ and $3.54 \rightarrow 0.76$. This was done by assuming various choices of spin for the 3.54 level, allowing all possible values of the two mixing ratios, and by using the measured branching ratio. The results showed that only $J=\frac{1}{2}$ and $J=\frac{3}{2}$ are possible spin assignments. The lack of a ground-state transition suggests but does not rigorously prove that $J=\frac{1}{2}$ is the most probable spin assignment since the ground-state spin of $\frac{5}{2}$ would require $L>2$ for the γ radiation.

G. The 3.80-MeV Level

The study of the $(\alpha$-$\gamma)$ angular correlation for the level at 3.80 MeV was complicated by experimental difficulties both in regard to the small yield of α_8 and because of the proximity to the α_7 group in the particle spectrum. Since the α_8 group was so much smaller than its neighbor α_7 (see Fig. 2), the contamination from the low-energy side of α_7 as well as any small target contaminant could appreciably distort the γ spectrum. Unfortunately, the small yield of α_8 did not allow a reliable correlation measurement.

The summed spectrum is shown in Fig. 15 measured with an incident He^3 energy of 7.0 MeV. Three primary branches through the 0.96- and 0.78-MeV levels and to the ground state are suggested by the results. This conclusion must be considered as tentative since the area between channels 15 and 35 has so few counts that no attempt could be made to interpret this region in terms of other weak branching schemes. Branching ratios were calculated assuming only three branches by measuring the areas under the full-energy-loss peaks for the $3.80 \rightarrow 0$ and $0.96 \rightarrow 0$, and the $0.78 \rightarrow 0$

transitions. Because of the poor statistics, the subtraction of the high-energy γ rays from under the 0.78- and 0.96-MeV photopeaks caused errors of about 30 to 40%. Using the least-squares method explained in Sec. IVF, the results were (80±10), (11±4), and (9±4)% for the 3.80 → 0, the 3.80 → 0.96, and the 3.80 → 0.78 transitions, respectively. Since the 3.80-MeV level appears to branch through the $\frac{3}{2}$ level at 0.96 MeV, the $\frac{1}{2}$ level at 0.78 MeV, and $\frac{5}{2}$ ground state, a spin assignment of $J=\frac{3}{2}$ would be consistent with the trend followed by all the lower levels of Si^{27}, for which no $L=2$ γ transitions were observed except those mixed with strong $L=1$ γ transitions.

H. The 4.13-MeV Level

The possibility of a level at 4.13 MeV was suggested by Hinds and Middelton[14] from their analysis of the $Si^{28}(He^3,\alpha)Si^{27}$ reaction using a magnetic spectrograph. The uncertainty was due primarily to contamination α groups from oxygen. However, the conditions under which the current data were taken, i.e., observing the α groups at 180° with an incident He^3 energy of 7.0 MeV, have separated the oxygen and silicon groups enough so that this α group was determined to belong to the Si^{27} spectrum.

TABLE I. Comparison of measured and calculated transition properties for Si^{27}. Experimental values are from this work. The procedures for the model calculations are given in the text. The $\frac{5}{2}$ spin refers to the ground state except where specifically designated by an asterisk.

Transition	Rotational	Core ($0^+,2^+$)	Core ($0^+,2^+,4^+$)	Observed
$E2/M1$ ratio				
$\frac{7}{2} \rightarrow \frac{5}{2}$	−0.27	−0.46	−0.35	−0.43±0.03
$\frac{5}{2} \rightarrow \frac{3}{2}$	0.22	−0.05	−0.12	−0.06±0.04
$\frac{3}{2} \rightarrow \frac{5}{2}$	~0.01	0.15	0.09	0.36±0.03
$(\frac{5}{2})^* \rightarrow \frac{5}{2}$	~0.01	0.63	0.34	−0.47±0.2
Width ratio				
$\Gamma[(\frac{5}{2})^* \rightarrow \frac{3}{2}]/\Gamma(\frac{5}{2})^*$	0.63	0.74	0.58	0.80±0.05

Figure 16 shows the summed γ-ray spectrum for the decay of the 4.13-MeV level. The branching is completely through the first and second excited states. The relative transition probabilities were calculated using the method explained in Sec. IVF, and the results were (90±10) and (10±3)% for the 4.13 → 0.78 and the 4.13 → 0.96 transitions, respectively. The angular distribution of the 4.13 → 0.78 transition with a 10% mixture of the 4.13 → 0.96 decay was isotropic to within 1.5%. Due to the weakness of the 0.96 → 0 decay, a reliable correlation could not be measured. The isotropy of the 4.13 → 0.78 and the decay through $J=\frac{1}{2}$ and $J=\frac{3}{8}$ levels are arguments for a probable $J=\frac{1}{2}$ spin assignment. However, a possible $J=\frac{3}{2}$ cannot be ruled out with the available data in any rigorous manner.

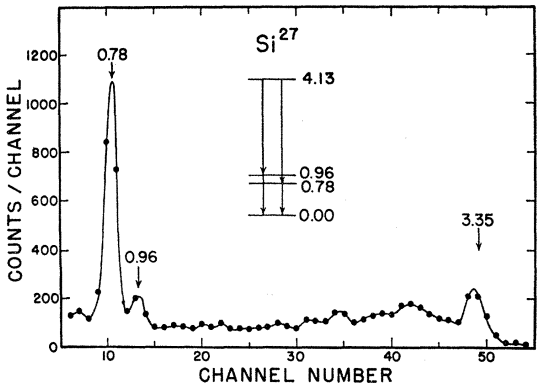

FIG. 16. Spectrum of γ rays summed over five angles in coincidence with the α group populating the Si^{27} 4.13-MeV level in the $Si^{28}(He^3,\alpha)Si^{27}$ reaction at a He^3 energy of 7.0 MeV. The γ-ray peaks correspond to the decay scheme shown. The random coincidences have been subtracted.

V. DISCUSSION AND COMPARISON WITH THEORY

The decay scheme of Si^{27} resulting from the evidence presented in Sec. IV and from previous work[14–16] is shown in Fig. 17 and listed in Table I. For those levels which are shown with two possible spin assignments, one enclosed with brackets and one not, the bracketed spin has not been rigorously excluded. The positive parities enclosed with brackets have not been rigorously determined by this experiment, but are strongly implied by relatively large quadrupole-dipole mixtures. Agreement in regard to the spins and the excitation energies of the low-lying levels of the mirror pair Si^{27}-Al^{27} was expected from the fact that the spacing between the Si^{27} levels are, with one exception, greater than any expected Coulomb energy shifts due to the different proton configurations. Based on information obtained from other mirror nuclei in this mass region, these shifts are expected to be less than about 150 keV.[29] A decay scheme for Al^{27} based on data as summarized

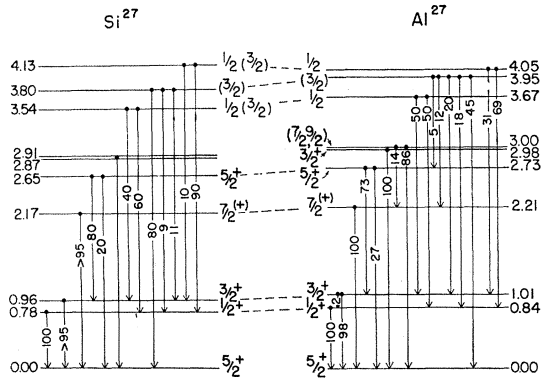

FIG. 17. Summary of spin assignments and γ-ray decay schemes for Si^{27} and Al^{27}. The Si^{27} data are from the present work and Refs. 14–16. The Al^{27} data are from summaries given in Refs. 19 and 29. The parentheses indicate uncertain assignments.

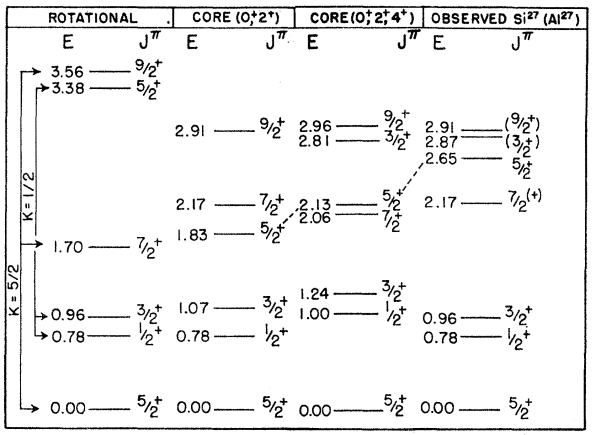

FIG. 18. Model predictions for the spin, parity, and level positions of the Si^{27} levels below 3.00 MeV. Model types are indicated across the top of the figure. A discussion of the calculations is given in the text. Observed levels for Si^{27} are shown on the extreme right. Level assignments enlcosed in parentheses are taken from the mirror nucleus Al^{27}.

by Wakatsuki *et al.*[19] is also shown in Fig. 17 for comparison with Si^{27}. Agreement between the mirror pair in regard to the electromagnetic decay properties is not necessarily expected since the transition amplitudes depend upon the electric charge and the magnetic moment of the odd particle in Al^{27} or Si^{27}.

The results of this experiment which indicate relatively large $E2/M1$ mixing ratios for the γ-ray decay of some of the low-lying levels of Si^{27} suggest, as was expected, a collective component in these levels. On the other hand, the work of Swenson *et al.*[16] and Hinds and Middleton[14,15] also indicates a significant single-particle component for some of these same levels. A physical picture which would be consistent with this information would be the separation of the motion of the last odd nucleon from that of the remaining "core". In the discussion that follows, the results of this experiment are compared with calculations based upon both the Nilsson model (axially symmetric Si^{28} core) and the excited-core model (Si^{28} excited core) to determine which model is more valid for Si^{27}.

A. Nilsson Model

In the case of the simple rotational or Nilsson model, the odd particle (hole) is assumed to be strongly coupled to an axially symmetric ellipsoid with a fixed deformation η and inverse moment of inertia $\hbar^2/2\mathcal{I}$. The solutions for this motion calculated for a harmonic-oscillator potential well having a spin orbit term with strength κ and an angular-momentum depression term with strength μ were first obtained by Nilsson.[20] To a first approximation, the projection K of the particle (hole) angular momentum on the nuclear symmetry axis is a constant of the system. Since the particle (hole) is strongly coupled to the core, it follows the core adiabatically, and the entire system rotates with an angular momentum $\mathbf{I}$. Such a motion manifests an $E=(\hbar^2/2\mathcal{I})\mathbf{I}\times(\mathbf{I}+1)$ energy dependence superimposed upon the energy levels of the particle (hole) itself.

The energy levels and spins for the Si^{27} nucleus are very similar to those of Al^{27}. Therefore, the choices of K and values for κ, μ, and η which have already been calculated for Al^{27} should apply approximately to Si^{27} as well. Several calculations, for example those by Bhatt[4] and Newton[21] have already been made for Al^{27}. Bhatt's parameters for Al^{27} which are consistent with values for other $1d$-$2s$ nuclei are $\kappa=0.1$, $\mu\simeq 0.3$, and $\eta\simeq 3$. The inverse moment of inertia was taken as 300 keV to agree with the 1.77-MeV spacing between the 0+ and the 2+ states of Si^{28}.

The energy levels labeled rotational in Fig. 18 are the results of a calculation made with these parameters under the assumption that the ground state is the first member of a $K=\frac{5}{2}$ band based on the Nilsson orbit 5 and that the level at 0.78 MeV is the first member of the $K=\frac{1}{2}$ band (orbit 9). The $J=\frac{7}{2}^+$ level at 1.70 MeV is predicted to lie somewhat lower than the experimentally determined $\frac{7}{2}$ level at 2.17 MeV. The next member of the $K=\frac{5}{2}$ band is the $J=\frac{9}{2}^+$ state which is predicted to occur at 3.56 MeV. While no $J=\frac{9}{2}$ level is known in Si^{27} Towle and Gilboy[22] and Lowergren[23] assign a spin of $\frac{9}{2}$ to the Al^{27} level at 3.00 MeV. Because of the excellent agreement observed between the mirror pair Si^{27}–Al^{27}, it is expected that the 2.91-MeV level, or possibly the 2.87-MeV level, will also have a spin of $\frac{9}{2}$. With a value for the decoupling parameter of $a\simeq -0.6$ the second member of the $K=\frac{1}{2}$ band agrees with the experimentally determined $J=\frac{3}{2}$ level at 0.96 MeV. As with the ground-state band, the third member of this band lies too high at 3.78 MeV.

Recently Wakatsuki and Kern[24] have made measurements suggesting that the spin of 3.00-MeV level in Al^{27} is $\frac{7}{2}$ instead of $\frac{9}{2}$. However, their assumption that the 3.00-MeV–to–ground-state transition $(\frac{7}{2})\rightarrow\frac{5}{2}$ occurs via pure $E2$ is not consistent with other $\Delta J<2$ transitions proceeding from the other levels in Al^{27}. For all these $\Delta J<2$ transitions, whether interband or intraband, the $E2$ widths are less than 25% of the corresponding $M1$ widths. A summary of these measurements is given in the work by Thankappan.[5] If this level at 3.00 MeV has $J=\frac{7}{2}$, Wakatsuki suggests it could be the fourth member of the $K=\frac{1}{2}$ band. This also seems to conflict with the fact that all the γ transitions from this level do not decay through the $K=\frac{1}{2}$ band, but instead decay through the neighboring members of the proposed $K=\frac{5}{2}$ band.[24,19] Although it

[19] T. Wakatsuki, Y. Hirao, I. Miura, and A. Shimizu, J. Phys. Soc. Japan **21**, 834 (1966).
[20] S. G. Nilsson, Kgl. Danske Videnskab. Selskab, Mat. Fys. Medd **29**, No. 16 (1955).
[21] T. D. Newton, Chalk River Report No. CRT-886, 1960 (unpublished).
[22] J. H. Towle and W. B. Gilboy, Nucl. Phys. **39**, 300 (1962).
[23] B. T. Lawergren, Nucl. Phys. **53**, 417 (1964).
[24] T. Wakatsuki and B. D. Kern, Bull. Am. Phys. Soc. **11**, 509 (1966).

appears that the spin assignment for the 3.00-MeV level in Al^{27} is not settled, a spin of $\frac{9}{2}$ will be assumed in the remainder of this discussion.

As already pointed out, for example, by Kelson and Levinson,[25] changing the moment of inertia separately for each band will improve the fit to the experimentally observed levels. This would mean that the rigidity or stability of the core is not a good approximation. They also point out that any coriolis term which would cause interference between members of the two bands would be very small. Since band mixing does not occur between the $K=\frac{5}{2}$ and $K'=\frac{1}{2}$ bands ($K-K'\neq 1,0$), band mixing would have to occur via bands lying higher than 3 MeV. This mixing is not likely to have a great effect on the positions of the low-lying levels.

The transition amplitudes can be calculated from the formulas given, for example, by Nilsson[20] and Davidson.[26] These equations were obtained by calculating the appropriate multipole operator in the body fixed system with axial symmetry and then transforming the result into the laboratory system with the usual rotational operator. The effective odd neutron charge is taken as $Ze/A^2\approx 0.018e$ and the magnetic moment of Si^{27} as $\mu=g_s\mathbf{S}+g_l\mathbf{I}+g_R\mathbf{R}$ where the first two terms are the odd particle (hole) contributions and the $g_R\mathbf{R}(g_R=Z/A=0.5)$ is the core contribution. The results of the calculations, using the formulas for the transition amplitudes, show two selection rules pertinent to the Si^{27} data. First, $M1$ transitions are forbidden between bands where $K-K'=2$. Second, the collective component in $E2$ transitions only exists where $K=K'$. Thus, to calculate $E2$ and $M1$ amplitudes it is necessary to consider mixing via the first $K=\frac{3}{2}$ band, Nilsson orbit 8, which would be located at approximately 4.5 MeV (using $\eta\approx 3.0$, $\kappa=0.05$ and $\mu\approx 0.3$). The inclusion of this band causes each unperturbed band to contain small components of the other two bands. The amplitudes for each band were found by diagonalizing the Hamiltonian given, for example, by Davidson.[26] However, band mixing was included only in the interband-transition calculations. The results are given in Table I in the column labeled rotational. The experimentally observed γ-ray energies were used in these calculations where an energy dependence was called for. It is evident that the magnitude of the interband transition mixing ratios $\frac{3}{2}\rightarrow\frac{5}{2}$, $(\frac{5}{2})^*\rightarrow\frac{5}{2}$ are not accounted for by this treatment. (The asterisk indicates the $J=\frac{5}{2}$ excited state.) The predicted mixing ratio for the $K=\frac{1}{2}$ band transition $(\frac{5}{2})^*\rightarrow\frac{3}{2}$ also disagrees with the measured value while the $K=\frac{5}{2}$ band $\frac{7}{2}\rightarrow\frac{5}{2}$ transition mixing ratio $x=-0.27$ is in reasonable agreement with the experimentally observed value of -0.43. The results for the $\Gamma[(\frac{5}{2})^*\rightarrow\frac{3}{2}]/\Gamma(\frac{5}{2})^*$ branching ratio of 63% is reasonable compared to the experimentally observed value of 80%. This branching-ratio calculation is sensitive to the degree of interband mixing and suggests that the $K=\frac{3}{2}$ orbit 8 mixture into $K=\frac{1}{2}$ orbit 9 and the $K=\frac{5}{2}$ orbit 5 was approximately correct. The calculation, however, is not sensitive to the $E2$ width since the $E2$ width is considerably smaller than the $M1$ width. Apparently, the underestimation of the interband $E2/M1$ ratios is due primarily to an underestimation of $B(E2)$ amplitudes rather than an overestimation of the $B(M1)$ amplitudes. This underestimation appears frequently in the $1d2s$ shell as evidenced by a summary of such values given in Table II.

TABLE II. Comparison of calculated and measured interband transition probabilities in Mg^{25}, Al^{27}, and Si^{27} nuclei. The calculations were based upon a rotational model as discussed in the given references. The $\frac{5}{2}$ spin refers to the ground state except where specifically designated by an asterisk.

Measurement	Transition	Nucleus	Rotational	Experiment	Reference
$B(E2)$I	$\frac{5}{2}\rightarrow\frac{3}{2}$	Mg^{25}	0.005	0.03	4
	$\frac{5}{2}\rightarrow\frac{3}{2}$	Al^{27}	0.05	0.3	4
	$\frac{5}{2}\rightarrow\frac{1}{2}$	Al^{27}	0.06	0.2	4
$E2/M1$	$\frac{3}{2}\rightarrow\frac{5}{2}$	Mg^{25}	0.03	0.3	4
	$\frac{3}{2}\rightarrow\frac{5}{2}$	Al^{27}	-0.1	-0.3	4
	$\frac{3}{2}\rightarrow\frac{5}{2}$	Si^{27}	~ 0.01	0.4	This work
	$(\frac{5}{2})^*\rightarrow\frac{5}{2}$	Si^{27}	~ 0.01	-0.5	This work

B. Excited-Core Model

Whereas in the rotational model the core is pictured as a static ellipsoid, in the excited-core approach the geometrical restrictions are relaxed and the empirical data of the Si^{28} core is emphasized. This is the advantage of the method in that the exact nature of the core states is not specified and, in principle, more complicated core excited states can be considered than can be done with a more specific model. As pointed out by Thankappan and True,[7] the present approach is more valid if the lowest core states are highly collective in nature. The large $B(E2)$ for the $2+\rightarrow 0+$ transition in Si^{28}, which is about 14 times the single particle estimate, suggest collective motion as do the large $E2/M1$ mixing ratios for the transitions in Si^{27}.

The initial calculations for the level positions and for the transition probabilities follow the procedures outlined by Thankappan[5] and Thankappan and True[7] in which a neutron hole state is coupled to the 0+ ground state and to the 2+ first excited state of Si^{28}. Harmonic-oscillator wave functions are used to represent the hole state $|j_p^{-1}\rangle=|\frac{5}{2}\rangle$. The only information necessary for the core wave function $|J_c\rangle$ is the energy of the 2+ level (1.77 MeV) and the $2+\rightarrow 0+$ transition strength ($65e^2f^4$). Obviously, the eigenvalues of the simple product wave function $|J_c\rangle|j_p\rangle$ would be degenerate at 1.77 MeV. Following Thankappan and True,[7] the scalar interaction

$$H_{\text{int}}=-\xi\mathbf{j}_p{}^{(1)}\cdot\mathbf{J}_c{}^{(1)}-\eta\mathbf{Q}_p{}^{(2)}\cdot\mathbf{Q}_c{}^{(2)}, \qquad (6)$$

[25] I. Kelson and C. A. Levinson, Phys. Rev. **134**, 269 (1964).
[26] J. P. Davidson, Rev. Mod. Phys. **1**, 105 (1965).

is introduced to represent the coupling between the hole and the core. The total-angular-momentum operators for the core and hole (particle) are $\mathbf{J}_c$ and $\mathbf{j}_p$, respectively the quadrupole moment operators are $\mathbf{Q}_c$ and $\mathbf{Q}_p$, and ξ and η are the parameters describing the strength of the interactions. The amplitudes for each component of the mixed hole and core states in the Si^{27} levels are found by diagonalizing H_{int}. The three parameters of the model were determined by fitting to the three energy differences $E_{1/2}-E_{5/2}$, $E_{7/2}-E_{1/2}$, and $E_{9/2}-E_{7/2}$. This led to the values $\chi_1=0.465$ MeV F^{-2}, $\chi_2=0.039$ MeV F^{-2}, and $\xi=-0.175$ MeV, where $\chi_1=\eta\langle 0\|\mathbf{Q}_c^{(2)}\|2\rangle$ and $\chi_2=\eta\langle 2\|\mathbf{Q}_c^{(2)}\|2\rangle$. The energy levels resulting from these calculations are shown in Fig. 18 under the caption core $(0^+,2^+)$. The $J=\frac{3}{2}$ and $J=\frac{5}{2}$ excited levels are the two levels predicted by the choice of χ_1, χ_2, and ξ. The $J=\frac{5}{2}$ level predicted at 1.83 MeV is in conflict with the experimentally observed one at 2.65 MeV. The corresponding wave functions for the only core-mixed states are given by

$$|\tfrac{5}{2}\rangle=0.92|0,\tfrac{5}{2};\tfrac{5}{2}\rangle+0.39|2,\tfrac{5}{2};\tfrac{5}{2}\rangle,$$
$$|(\tfrac{5}{2})^*\rangle=-0.39|0,\tfrac{5}{2};\tfrac{5}{2}\rangle+0.92|2,\tfrac{5}{2};\tfrac{5}{2}\rangle,$$

where $|J_c,j_p;I\rangle$ represents a state of total spin I obtained by coupling the $d_{5/2}^{-1}$ neutron hole to a core state of spin J_c.

Using these wave functions, transition amplitudes were calculated again assuming, as in the Nilsson model calculations, independent particle (hole) and core contributions. The expression for the magnetic moment was taken to be the same as that used for the rotational model, and the effective neutron charge was assumed to be zero. (The Z/A^2 value used in the Nilsson model would not appreciably change any of the results.) The gyromagnetic ratio was taken as 80% that of a free neutron (see Ref. 5). Since the multipole operators are assumed to be the sum of the core and single hole operators, the matrix elements for the transition strengths can be calculated by recoupling the angular momenta.

The results for the transition amplitudes are given in Table II in the column labeled core $(0^+,2^+)$. Agreement with experiment is reasonable except for the $(\frac{5}{2})^*\rightarrow\frac{5}{2}$ ratio. The $\frac{3}{2}\rightarrow\frac{5}{2}$ ratio is somewhat low, but this could be due to overestimation of $B(M1)$. In the case of Al^{27}, Thankappan[5] found that the $\Gamma(M1)$ value for the $\frac{3}{2}\rightarrow\frac{5}{2}$ transition was about five times too large compared with the observed value. The small value for the $(\frac{5}{2})^*\rightarrow\frac{3}{2}$ mixing ratio ($x=-0.04$) is the consequence of the fact that both levels in the transition are primarily coupled to the 2^+ Si^{28} level. Thus the Si^{28} $2^+\rightarrow 0^+$ transition contribution is highly suppressed in the $(\frac{5}{2})^*\rightarrow\frac{3}{2}$ Si^{27} transition. The disagreement in the sign of the $(\frac{5}{2})^*\rightarrow\frac{5}{2}$ ratio is not trivial, but this ratio is more sensitive to the degree of 0^+ and 2^+ core states present in the decaying level than any of the other mixing ratios. The branching ratio $\Gamma[(\frac{5}{2})^*\rightarrow\frac{3}{2}]/\Gamma(\frac{5}{2})^*$ also involves this decay but is primarily dependent on the $B(M1)$ calculations. The accuracy with which the core model predicted this 80% branching ratio suggests an accuracy in the $\Gamma(M1)$ values involved.

Thankappan attempted to improve the predictions for the $B(M1)$ values for transitions in Al^{27} by including more terms in the scalar interaction H_{int}. However, the transition probabilities were not appreciably different from those calculated assuming the H_{int} given in Eq. (6). Recently, Evers *et al.*[27] recalculated some of the transition strengths for Al^{27} by extending the excited core-model wave functions to include a mixture of the two $\frac{3}{2}^+$ states at 1.013 MeV and at 2.98 MeV. The second state, which is not accounted for by the extreme excited-core model, was interpreted as due to the single-particle excitation $(d_{5/2})^{-2}d_{3/2}$ coupled to the ground state of Si^{28}. Their results indicated that small single-particle admixtures can account for the discrepancy of the earlier calculation, in the $\frac{3}{2}\rightarrow\frac{5}{2}$ mixing ratio, due to the interference between the two $\frac{3}{2}$ wave functions. Another approach would be to allow higher excitations of the core to enter the wave function. A calculation was done which couples a $d_{5/2}$ hole to the 0^+ ground state, the 2^+, 1.77-MeV level and the 4^+, 4.61-MeV level in Si^{28}.

To calculate the degree of mixing, the reduced matrix elements $\langle J_c\|\mathbf{Q}_c^{(2)}\|J_c'\rangle$ for the quadrupole operator must be estimated between the core states $\mathbf{J}_c$ and $\mathbf{J}_c'$. The matrix element $\langle J_c\|\mathbf{Q}_c^{(2)}\|J_c\rangle$ is proportional to the quadrupole moment of the corresponding Si^{28} level. Since Si^{28} is a doubly closed $d_{5/2}$ shell nucleus its quadrupole moments are expected to be small; therefore, the approximation that $\langle J_c\|\mathbf{Q}_c^{(2)}\|J_c\rangle=0$ was made. Indeed, the results of the earlier calculation give $\chi_2/\chi_1=\langle 2\|\mathbf{Q}_c\|2\rangle/\langle 0\|\mathbf{Q}\|2\rangle\simeq 0.08$. The remaining values of $\langle J_c\|\mathbf{Q}_c^{(2)}\|J_c'\rangle$ can be estimated from the $B(E2)$ values as determined from lifetime measurements[28] of the 4^+, 4.61-MeV level of Si^{28}. Assuming that the $4^+\rightarrow 2^+$ transition is pure $E2$, it was calculated that $\langle 2\|\mathbf{Q}_c\|4\rangle=30.2f^2$. The result for the energy levels are shown in Fig. 18 under the heading core $(0^+,2^+,4^+)$. The two model parameters used were $\xi=-0.20$ MeV and $\eta=\pm 0.04$ MeV F^{-4} (i.e. $\chi_1=\eta\langle 0\|\mathbf{Q}_c\|2\rangle=0.72$ MeV F^{-2}). The over-all agreement with the experimentally determined levels is better than in the simpler excited-core calculation, and in particular, the $(\frac{5}{2})^*$ level is calculated to be at 2.13 MeV which is nearer the known $(\frac{5}{2})^*$ level at 2.65 MeV. Also the results suggest that the level observed at 2.87 MeV is the lowest $\frac{3}{2}^+$ level of the multiplet from the 4^+ core state. While the spin of this state in Si^{27} has not been assigned, a spin and parity of $\frac{3}{2}^+$ has been determined for the mirror level in Al^{27} at 2.98 MeV.[22,29] Higher levels with $J>\frac{3}{2}$ are, of course,

[27] D. Evers, J. Hertel, T. W. Retz-Schmidt, and S. J. Skorka, in *Proceedings of the International Conference on Nuclear Physics, Gatlinburg, 1966* (Academic Press Inc., New York, 1967), contributed paper 5.27.

[28] S. W. Robinson, R. D. Bent, and T. R. Canada, Bull. Am. Phys. Soc. **10**, 525 (1965).

[29] P. M. Endt and C. Van der Leun, Nucl. Phys. **34**, 1 (1962).

predicted as the remaining multiplets of the 4^+ levels. These levels lie at energies >4 MeV and are not relevant to this experiment. The wave functions for the $\frac{5}{2}$ ground state and for the first six excited states are given by

$$
\begin{aligned}
|\tfrac{5}{2}\rangle &= 0.85|0,\tfrac{5}{2};\tfrac{5}{2}\rangle+0.52|2,\tfrac{5}{2};\tfrac{5}{2}\rangle+0.10|4,\tfrac{5}{2};\tfrac{5}{2}\rangle,\\
|\tfrac{1}{2}\rangle &= |2,\tfrac{5}{2};\tfrac{1}{2}\rangle,\\
|\tfrac{3}{2}\rangle &= 0.98|2,\tfrac{5}{2};\tfrac{3}{2}\rangle+0.19|4,\tfrac{5}{2};\tfrac{3}{2}\rangle,\\
|\tfrac{7}{2}\rangle &= 0.90|2,\tfrac{5}{2};\tfrac{7}{2}\rangle+0.43|4,\tfrac{5}{2};\tfrac{7}{2}\rangle,\\
|(\tfrac{5}{2})^*\rangle &= -0.51|0,\tfrac{5}{2};\tfrac{5}{2}\rangle+0.74|2,\tfrac{5}{2};\tfrac{5}{2}\rangle+0.43|4,\tfrac{5}{2};\tfrac{5}{2}\rangle,\\
|(\tfrac{3}{2})^*\rangle &= -0.19|2,\tfrac{5}{2};\tfrac{3}{2}\rangle+0.98|4,\tfrac{5}{2};\tfrac{3}{2}\rangle,\\
|\tfrac{9}{2}\rangle &= 0.90|2,\tfrac{5}{2};\tfrac{9}{2}\rangle+0.43|4,\tfrac{5}{2};\tfrac{9}{2}\rangle.
\end{aligned}
$$

Using the above wave functions, the transition strengths were again calculated. The results are shown in Table I under the heading "Core $(0^+,2^+,4^+)$". The particular problem with the underestimation of the $\frac{3}{2}\rightarrow\frac{5}{2}$ ratio is, unfortunately, not solved by the inclusion of the 4^+ core level. In fact the $\Gamma(M1)$ value (not shown in the table) actually increases as the core wave functions are mixed into the 0.96-MeV and ground-state wave functions. Also the sign error in regard to the $(\frac{5}{2})^*\rightarrow\frac{5}{2}$ transition was not corrected. Apparently, the inclusion of the $|4^+,\frac{5}{2}\rangle$ configuration, although a natural one, is not the most important correction to the $|2^+,\frac{5}{2}\rangle$ configuration within the framework of the excited-core model.

VI. CONCLUSION

Although the spins of the low levels of Si^{27} can at least be understood qualitatively by a Nilsson picture, it appears that the shortcomings of the rotational model approach could be its neglect of more complicated intrinsic motion, perhaps in the form of a collective core excitation. The results in Table II as well as further calculations and experimental information on interband transitions may indicate a similar problem in other $1d$-$2s$ shell nuclei. Bar-Touv and Kelson[30] have already pointed out this problem in the γ transitions of Al^{25} and Mg^{25}. Furthermore, their Hartree-Fock calculations indicate that Si^{28} appears to be in a region in which the sign of the nuclear deformation is changing. The asymmetric-core approach of Chi and Davidson[31] could directly enhance $B(E2)$ matrix elements in $\Delta K=2$ transitions but not $\Delta K=1$. However, considering small, time-dependent vibrations about a deformed equilibrium position of the nucleus as done by Faessler[32] may account for both $\Delta K=2$ and $\Delta K=1$ cases. $B(E2)$ values could also be enhanced by assuming an effective charge much greater than the recoil term (Z/A^2) which was used here or by assuming a charge polarization of the core by the odd neutron. Bhatt[4] used an effective proton charge of $(1+Z/A)e=1.5e$ and suggested a neutron charge of $(Z/A)e$, but this still did not account for the measured values of $B(E2)$ and $E2/M1$ in Al^{27} and Mg^{25} interband transitions.

The excited-core approach, however, was able to account approximately for the energy levels and most of the transition properties with essentially two arbitrary parameters, the dipole and quadrupole particle-core coupling strengths. This implies that the particle-core interaction was relatively weak. That is, the interaction did not mix the Si^{28} levels of the core to the extent that the identity of these levels was lost in the odd-A nucleus. Even after the 4^+ and 0^+ levels of Si^{28} were allowed to enter the Si^{27} wave functions, all the original 2^+ multiplet $(J=\frac{1}{2},\ \frac{3}{2},\ (\frac{5}{2})^*,\ \frac{7}{2},\ \frac{9}{2})$ remained primarily $|2,\frac{5}{2};J\rangle$. Si^{28} is a doubly closed $d_{5/2}$ subshell. It may be of interest to investigate whether this somewhat "weak" coupling is a property of nuclei which can be viewed as a closed subshell plus particle or hole. Additional calculations on Al^{27} and other $1d$-$2s$ nuclei are presently being carried out.

ACKNOWLEDGMENTS

We should like to thank Dr. Max Huber for his enlightening discussions concerning the interpretations of the data in terms of nuclear model calculations. Also, we wish to thank Dr. R. V. Poore, L. C. Haun, and V. H. Webb for their assistance in the acquisition of the data.

[30] J. Bar-Touv and I. Kelson, Phys. Rev. **138**, 1035 (1965).

[31] B. E. Chi and J. P. Davidson, Phys. Rev. **131**, 366 (1963).

[32] Amand Faessler, *Internal Conversion Processes* (Academic Press Inc., New York, 1966).